IOPscience iopscience.iop.org

Home Search Collections Journals About Contact us My IOPscience

Enhanced dopant solubility in strained silicon

This article has been downloaded from IOPscience. Please scroll down to see the full text article.

2004 J. Phys.: Condens. Matter 16 9117

(http://iopscience.iop.org/0953-8984/16/50/002)

View the table of contents for this issue, or go to the journal homepage for more

Download details:
IP Address: 129.252.86.83
The article was downloaded on 27/05/2010 at 19:27

Please note that terms and conditions apply.

INSTITUTE OF PHYSICS PUBLISHING JOURNAL OF PHYSICS: CONDENSED MATTER

J. Phys.: Condens. Matter **16** (2004) 9117–9126 PII: S0953-8984(04)86952-2

Enhanced dopant solubility in strained silicon

J Adey[1], **R Jones**[1] **and P R Briddon**[2]

[1] School of Physics, University of Exeter, Exeter EX4 4QL, UK
[2] Physics Centre, School of Natural Science, Newcastle upon Tyne NE1 7RU, UK

E-mail: adey@excc.ex.ac.uk

Received 22 September 2004, in final form 26 October 2004
Published 3 December 2004
Online at stacks.iop.org/JPhysCM/16/9117
doi:10.1088/0953-8984/16/50/002

Abstract
The effect of biaxial strain on the solubility of the common donor arsenic and acceptor boron is calculated using spin-polarized local density functional theory. The change in solubility with strain is considered in terms of contributions from the change in total energy and Fermi energy with strain. The solubility of boron is found to be enhanced by compressive biaxial strain due to a reduction in the total energy of the small substitutional impurity and an increase in the Fermi energy for compressive strain. The solubility of arsenic is shown to be enhanced by tensile strain and this is due entirely to the change in Fermi energy. For boron as well as arsenic the change in Fermi energy with strain is shown to make the dominant contribution.

1. Introduction

The continual reduction in device feature size demands an increase in dopant concentration along with a reduction in dopant diffusivity. Strain has the potential to control both dopant solubility and diffusivity. It has been demonstrated that biaxial strain introduced by growing Si epitaxially on SiGe can reduce the diffusivity of boron [1–3]. For arsenic the effect of biaxial strain on diffusion is, to our knowledge, yet to be investigated. Even less is known about the effect of strain on the solubility of dopants.

The effect of biaxial strain on the solubility of both the acceptor boron and donor arsenic has not been studied experimentally but the change in equilibrium solubility of boron with biaxial strain has been studied theoretically, by Sadigh *et al* [4]. Using local density functional theory (LDFT) Sadigh *et al* predicted that the equilibrium solubility of boron should be enhanced by $\sim$150% for a -1% biaxial strain at 1000 °C (we adopt the convention that tensile strains are positive and compressive ones negative). Sadigh *et al* showed that this enhancement is due to two effects. The variation of the Fermi energy with strain alters the stability of charged centres with respect to a neutral precipitate and the strain induced change in lattice constant will lead to increased stability and hence equilibrium concentration of dopants that tend to

induce a change in lattice constant of similar sense in unstrained material. As we confirm here, both of these effects enhance the solubility of boron in compressively strained material but it is the Fermi energy's variation with strain that dominates. The effect of strain on the solubility of the donor arsenic is considered here for the first time. Surprisingly (since arsenic has a larger atomic radius than silicon) the lattice constant of silicon is found to contract slightly with arsenic doping. This tends to increase the solubility of arsenic in compressively strained material in competition with the change in Fermi energy which tends to increase its solubility in tensile strained material. It is again the change in Fermi energy with strain which dominates and we show here that the solubility of arsenic should be enhanced by tensile strain.

2. Method

Total energy calculations have been performed using the AIMPRO LDFT pseudopotential code. Calculations were performed on supercells of various sizes but 64 atoms was found to be large enough to deliver converged results. To support this, in most figures data points from calculations performed using 216-atom supercells, which differ very little from those produced using the smaller cell, are shown. The larger cell corresponds to a dopant concentration of 2×10^{20} cm^{-3}. The Brillouin zone was sampled using a $2 \times 2 \times 2$ (2^3) Monkhorst–Pack (MP) sampling scheme [5]. The variation of the valence band maximum and conduction band minimum with strain is critical to this discussion. In bulk silicon, which has a two-atom unit cell, these points lay at the Γ point and along the Γ–X direction, close to the X point, respectively. However, here we have used a 64-atom unit cell and so the band structure of the primitive cell is folded onto itself several times resulting in a far more complicated band structure in which the valence band maximum and conduction band minimum occur at several points in the Brillouin zone. In this case a 2^3 MP sampling scheme gives converged values for the energy of the valence band maximum and conduction band minimum, evidenced by there being no difference in energy when the supercell size (and hence band folding) is increased from 64 to 216 atoms (see figure 1) nor any significant difference when the k-point sampling density is increased from 2^3 to 4^3 (not shown).

Since a charged defect that is periodically repeated in space results in an infinite Coulomb energy, a compensating background charge is applied to the supercell. However, quadrupole and higher order multipole interactions between supercells result in an error in the calculated total energy. There are schemes for correcting the total energy for these interactions but, as will be explained below, such corrections were not necessary here.

The effect of biaxial strain on the equilibrium solubility limit (ESL) is calculated following the method described by Sadigh *et al* ([4] and references therein), summarized below.

Inserting an impurity into an unstrained, perfect crystal leads to changes in the lattice constant and consequently induces strain in an epitaxial layer. The lattice parameter change is linear in dopant concentration and corresponds to a strain of -0.002 for boron concentrations around 4×10^{20} cm^{-3} [6, 7]. The biaxial strain that results from growing silicon on some lattice mismatched material such as Si_xGe_{1-x} is typically much larger than this and so we define the reference lattice constant to be the calculated lattice parameter of pure bulk silicon, a_0, which is found to be 5.39 Å and can be compared with an experimental value of 5.43 Å. For arsenic, we shall show that the change of lattice parameter with doping is very much smaller.

The effect of biaxial strain on pure silicon can now be found by imposing an in-plane, strained lattice parameter on a (001) slab of bulk silicon and relaxing the free cell parameter along the perpendicular [001] direction. Then the impurity atom is placed in this relaxed supercell and the atomic positions are relaxed for fixed lattice vectors. Re-relaxing the [001] cell parameter after the impurity was placed in the supercell had negligible effect on

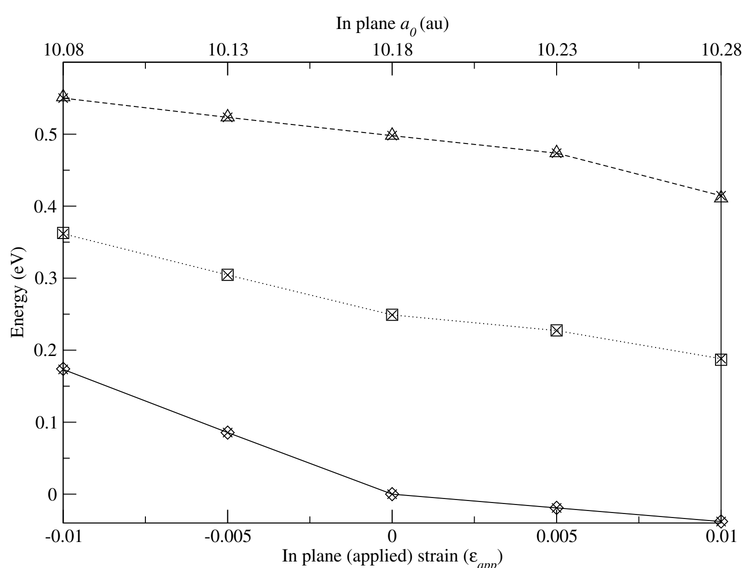

Figure 1. The energy of the valence band maximum, conduction band minimum and mid-gap energy as a function of tensile (positive) and compressive (negative) biaxial strain $\epsilon_{\rm app}$. Crosses joined by a solid line show the valence band maximum, crosses joined by a dashed line show the conduction band minimum and crosses joined by a dotted line show the mid-gap energy level ($E_{\rm mid}$) calculated using a 64-atom supercell. Using a 216-atom supercell the valence band maximum, conduction band minimum and $E_{\rm mid}$ have values shown by empty diamonds, triangles and squares respectively. Note the independence of these energies of supercell size.

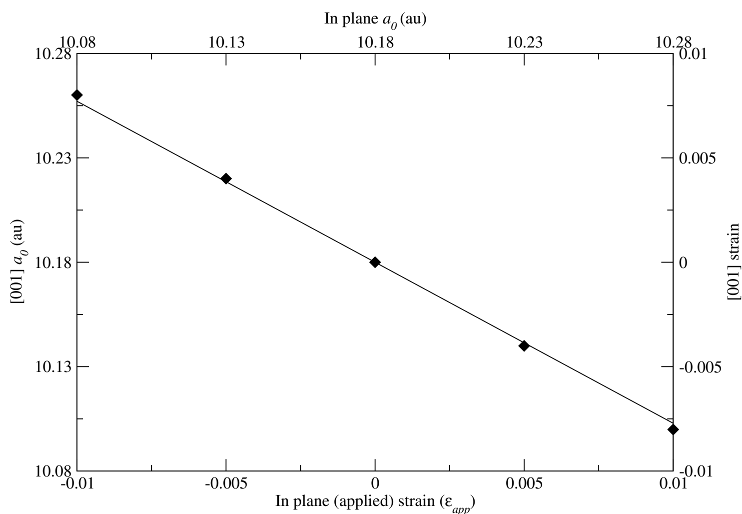

Figure 2. The variation of the relaxed [001] lattice constant with the biaxial strain. Data points are the calculated values while the line is a plot of the equation $\epsilon_{\rm rel} = -2(C_{12}/C_{11})\epsilon_{\rm app}$ given by elasticity theory.

the [001] cell parameter ($<$0.1 %) and total energy of the system ($<$0.5 meV). Figure 2 shows the calculated relaxed [001] lattice parameter in a 64-atom cell as a function of biaxial strain $\epsilon_{\rm app} = \epsilon_{[100]} = \epsilon_{[010]}$. The strain along [001] is $\epsilon_{\rm rel} = \epsilon_{[001]} = (a_{[001]} - a_0)/a_0$

and its variation is in excellent agreement with the expression derived from elasticity theory $\epsilon_{\rm rel} = -2(C_{12}/C_{11})\epsilon_{\rm app}$ shown by the line in figure 2, where C is the elastic stiffness tensor and C_{12} and C_{11} are the experimental elastic constants 6.39×10^{10} and 16.57×10^{10} N m^{-2} respectively [8].

The ESL of an isolated, charged substitutional dopant X_s is given in terms of its formation energy by

$$[{\rm X_s}] = A \exp\left(\frac{-E_{\rm f}}{kT}\right) \tag{1}$$

where k is Boltzmann's constant and T temperature. The value of A depends on the number of possible sites available for the substitutional dopant. This is taken to be constant since the change in the density of lattice sites is negligible for the small strains considered here. $E_{\rm f}$, the formation energy, is given by

$$E_{\rm f}(\epsilon_{\rm app}) = E_{\rm T}(\epsilon_{\rm app}) + qE_{\rm F}(\epsilon_{\rm app}) - \sum_s n_s \mu_s \tag{2}$$

where $E_{\rm T}$ is the total energy of the ionized substitutional dopant in a supercell, q is its charge state, $E_{\rm F}$ is the Fermi energy and n_s is the number of atoms of species s in the supercell which have chemical potential μ_s. The chemical potentials of both boron and arsenic, $\mu_{\rm B}$ and $\mu_{\rm As}$, are related to the energy of a dopant atom in its precipitate and are assumed to be independent of strain since it is likely that the structure and hence energy of a dopant atom within the precipitate would not depend upon the precise lattice constant of the bulk material. On the other hand, the chemical potential of silicon, $\mu_{\rm Si}$ varies with strain ($\epsilon_{\rm app}$) and is taken to be the total energy per atom of an n-atom supercell of biaxially strained pure silicon relaxed in the [001] direction ($\mu_{\rm Si}(\epsilon_{\rm app}) = E_{\rm T}^{\rm Si}(\epsilon_{\rm app})/n$).

The Fermi energy at high temperature is given by [9]

$$E_{\rm F}(\epsilon_{\rm app}) = E_{\rm mid}(\epsilon_{\rm app}) \pm kT\left[\ln\left|\frac{[{\rm X_s}]}{n_{\rm i}}\right| + \ln\left|\frac{1}{2}\left(1+\sqrt{1+\left(\frac{2n_{\rm i}}{[{\rm X_s}]}\right)^2}\right)\right|\right] \tag{3}$$

where $E_{\rm mid}$ is the energy midway between the valence band maximum and conduction band minimum in bulk silicon subject to biaxial strain $\epsilon_{\rm app}$. The second term in equation (3) is positive for donors and negative for acceptors. The value of $E_{\rm mid}$ is obtained from a Kohn–Sham band structure which gives a gap of 0.50 eV for unstrained material. The effect of quasi-particle corrections on the change in band gap with strain has been considered in [4] where it is shown to be negligible. This implies that the infamous underestimation of the band gap within local density functional theory is effectively independent of strain for small biaxial strains. Hence LDFT is able to predict the change in band gap with strain and thus the underestimation in the magnitude of the band gap does not affect this problem as will become apparent. The density of intrinsic carriers, $n_{\rm i}(\epsilon_{\rm app})$ in equation (3), is given by [9]

$$n_{\rm i}(T, \epsilon_{\rm app}) = \sqrt{N_{\rm v}N_{\rm c}} \exp\left(-\frac{E_{\rm gap}(\epsilon_{\rm app})}{2kT}\right) \tag{4}$$

where $N_{\rm v}$ and $N_{\rm c}$ are the effective densities of states in the valence and conduction bands respectively and $E_{\rm gap}$ is the size of the silicon (Kohn–Sham) band gap for the given strain. Again we stress that it is the *change* in band gap with strain that is important to this problem as will be explained below. We will take $N_{\rm v}$ and $N_{\rm c}$ to be constant with strain and temperature. The variation of the product of $N_{\rm v}$ and $N_{\rm c}$ with strain and temperature has been considered by Sadigh *et al* [4] and is found to make no significant differences to the results.

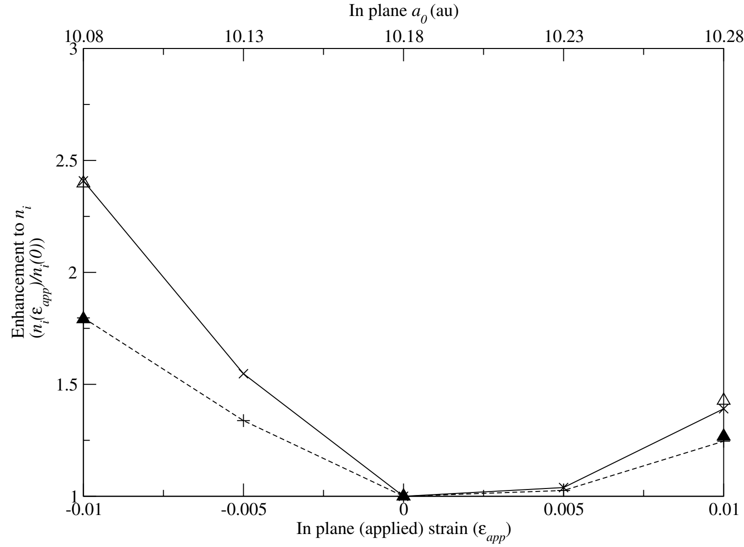

Figure 3. $n_{\rm i}(\epsilon_{\rm app})/n_{\rm i}(0)$ calculated using 64- and 216-atom supercells for two different temperatures. The crosses joined by a solid line and the plus signs joined by a dashed line are values calculated using 64-atom supercells for $T = 800$ and 1200 K respectively. Empty and filled triangles are the values calculated in 216-atom supercells for $T = 800$ and 1200 K respectively demonstrating the convergence with respect to cell size.

Taking the doping level into account through the Fermi energy, the ESL of the charged substitutional dopant is then given by the above equations. In the case where $n_{\rm i} \ll [{\rm X_s}]$, these equations are easily solved to give

$$[{\rm X_s}] = \sqrt{A n_{\rm i}(T, \epsilon_{\rm app})}\exp\left(\frac{-(E_{\rm T}(\epsilon_{\rm app}) - \sum_s n_s\mu_s) - qE_{\rm mid}(\epsilon_{\rm app})}{2kT}\right). \qquad (5)$$

Of interest here is the *enhancement* in the ESL with strain and for this the chemical potential of the dopant and $N_{\rm v}$ as well as $N_{\rm c}$ are not required, nor are the absolute values of $E_{\rm mid}$ or $E_{\rm gap}$. The enhancement in the ESL, $E(\epsilon_{\rm app}, T)$, is defined as $([{\rm X_s}](\epsilon_{\rm app}) - [{\rm X_s}](0))/[{\rm X_s}](0)$. This quantity can be more accurately calculated than the absolute ESL since many terms which are not easily calculated are cancelled. This is true of the artificial additional terms to the total energy which result from multipole interactions between charged supercells, since the enhancement depends on the change in total energy of a supercell containing the charged dopant with strain. Since this strain is small the supercells are almost identical and hence any multipole terms resulting from the computational treatment will be almost identical and therefore cancel.

3. Results

Figure 1 shows that $E_{\rm mid}(\epsilon_{\rm app})$ decreases almost linearly with biaxial strain $\epsilon_{\rm app}$. Since the Fermi energy is approximately equal to $E_{\rm mid}$ (equation (3)) this result implies that if the other terms are constant, a positively charged donor's solubility is enhanced by tensile strain while a negatively charged acceptor's solubility is enhanced by compressive strain. The enhancement to the equilibrium solubility is also proportional to $\sqrt{n_{\rm i}(\epsilon_{\rm app})/n_{\rm i}(0)}$. The dependence of $n_{\rm i}(\epsilon_{\rm app})/n_{\rm i}(0)$ upon strain is shown in figure 3 for two different temperatures. The number of

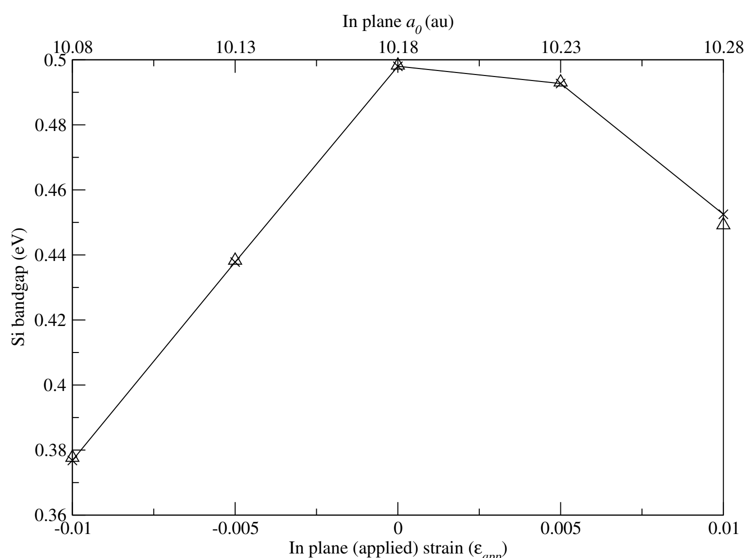

Figure 4. The Kohn–Sham band gap of silicon evaluated for 64-and 216-atom supercells as a function of biaxial strain ϵ_{app}. The solid line with crosses shows values calculated using 64-atom supercells while triangles show the values calculated using 216-atom supercells.

intrinsic carriers is increased for both negative and positive strains due to the narrowing of the band gap with strain of either sense (figure 4). Thus a study of strained, pure silicon alone predicts that the change in Fermi energy with strain will enhance the solubility of positively charged defects under tensile strain and negatively charged defects under compressive strain.

3.1. Boron

We now consider the effect of strain on the ESL of the acceptor boron. We first check whether the theory is able to account for the change in lattice parameter with boron doping concentration. This is done by first relaxing the contents, and then the volume, of a neutral 64-atom supercell containing a single substitutional boron atom. This yields a lattice parameter $a_0(\text{B})$ of 5.36 Å. The variation of this parameter is, according to Vegard's law, linear in boron concentration and this variation can be written as $(a_0(\text{B}) - a_0)/a_0 = \beta[\text{B}]$ where β is calculated to be -5.99×10^{-24} cm^3 in good agreement with the value -5.2×10^{-24} cm^3 found experimentally [6, 7]. The four silicon–boron bonds had lengths of 2.047 Å.

We now consider the effect of biaxial strain on a 64-atom cell containing a single substitutional boron atom. The calculated differences between the four silicon–boron bond lengths are found to be negligible, the strain being accommodated by an adjustment in bond angles. The silicon–boron bond length is shown in table 1 for different strains.

The variation of the formation energy of substitutional boron with strain has two main components: the variation in total energy and the variation in Fermi energy. Figure 5 shows the formation energy of B_s^- as a function of ϵ_{app} for a fixed Fermi energy (which demonstrates the variation in formation energy due to only the variation in total energy) and for a Fermi energy that is allowed to vary with strain. The formation energy in unstrained material is set to zero. This figure illustrates two points. The solubility of boron would be enhanced by compressive strain due to the change in total energy with strain alone. Including contributions to the change in formation energy from the change in Fermi energy with strain greatly increases this trend

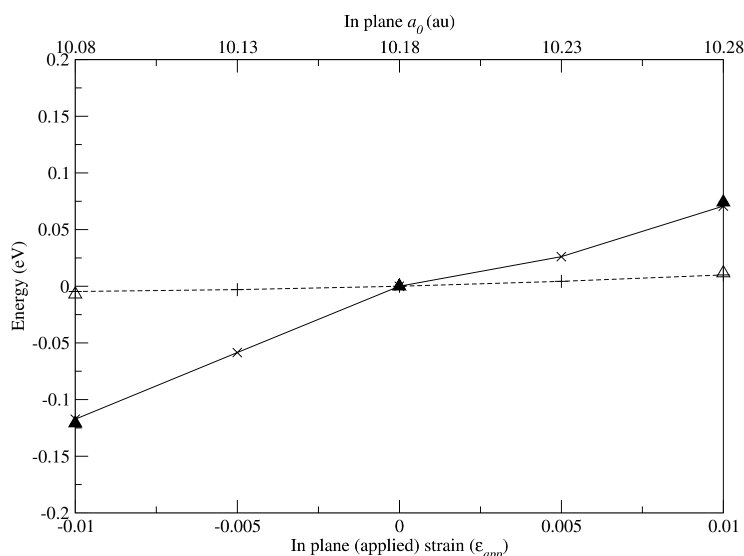

Figure 5. The formation energy of substitutional boron including and excluding the change in Fermi energy with strain. Plus signs joined by a dashed line and crosses joined by a solid line show values calculated using 64-atom supercells for the case where E_F is constant and where E_F varies with strain respectively. Empty triangles and filled triangles show the values where E_F is constant and where E_F varies with strain respectively calculated with 216-atom supercells to demonstrate convergence.

Table 1. The impurity bond length dependence upon biaxial strain. For comparison, the bond lengths in equivalently strained bulk silicon are also shown. The unit of length is the ångström. Note that all four bond lengths are equal and the strain is accommodated by a change in bond angle.

ϵ_{app}	Bulk	B	As
−0.01	2.324	2.050	2.387
−0.005	2.329	2.055	2.391
0	2.333	2.059	2.396
0.005	2.338	2.064	2.401
0.01	2.343	2.069	2.406

by reducing the formation energy for compressive strain and increasing it for tensile strain. This is seen in figure 6 which shows the enhancement to the equilibrium solubility limit for two different temperatures for the case where the Fermi energy is fixed (so the variation in stability comes entirely from the change in total energy) and the case where the Fermi energy varies with strain. This clearly illustrates that the change in Fermi energy with strain increases the predicted ESL by an order of magnitude.

3.2. Arsenic

The same analysis for is now performed for arsenic. A single neutral arsenic atom in a 216-atom supercell results in a relaxed lattice parameter a_0(As) of 5.388 Å. This gives a β value of -0.06×10^{-24} cm^3 in good agreement with the small negative value -0.1×10^{-24} cm^3 found experimentally [6, 11]. Using a smaller 64-atom supercell it is found that the lattice constant is identical to that of bulk material (i.e. $\beta = 0$). Details of the arsenic–silicon bond lengths have been found using EXAFS [10]. It is reported that, relative to the equivalent distance in pure

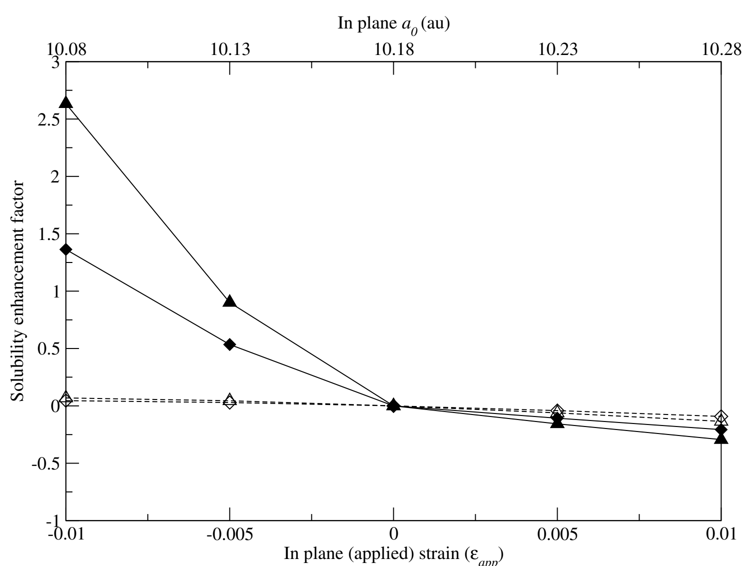

Figure 6. The enhancement to the equilibrium solubility of boron with strain for two different temperatures (triangles correspond to 800 K and diamonds correspond to 1200 K). To illustrate the influence of the change in Fermi energy the enhancement is shown for a Fermi energy set to be constant with strain (dashed lines and empty symbols) and for the value of E_F calculated as a function of strain (solid lines and filled symbols).

Table 2. A comparison of the change in first-, second-and third-nearest neighbour (NN) distances between Si and Si:As. EXAFS [10] and the present calculations agree that there is a dilation around the As atoms which drops of sharply and in fact leads to a *smaller* lattice constant than bulk Si. The theoretical values were calculated using volume relaxed, 216-atom supercells. Lengths are in units of ångströms.

	EXAFS			LDFT		
NN	Bulk	Si:As	Increase (%)	Bulk	Si:As	Increase (%)
1	2.351	2.43	3.36	2.333	2.397	2.71
2	3.840	3.87	0.78	3.810	3.822	0.32
3	4.502	4.53	0.62	4.468	4.479	0.25
4				5.389	5.397	0.15
5				5.872	5.875	0.05
6				6.600	6.602	0.04
7				7.000	7.003	0.05
8				7.620	7.619	−0.02

silicon, the distance between the arsenic atom and its first-nearest neighbour is ∼3% larger, decreasing to 0.78% larger and 0.62% larger for the second-and third-nearest neighbours and presumably becoming negative at larger distances to result in the measured overall reduction in lattice constant. Our calculations agree well with these EXAFS data as shown in table 2 and we predict that the distance between arsenic and its ∼8th-nearest neighbour is indeed shorter than the distance between equivalent crystal sites in bulk silicon.

Next we discuss the effect of biaxial strain on the ionized dopant. The arsenic–silicon bond lengths in biaxially strained material are given in table 1. The calculated change in formation energy due to the change in total energy and the combination of the change in total energy and

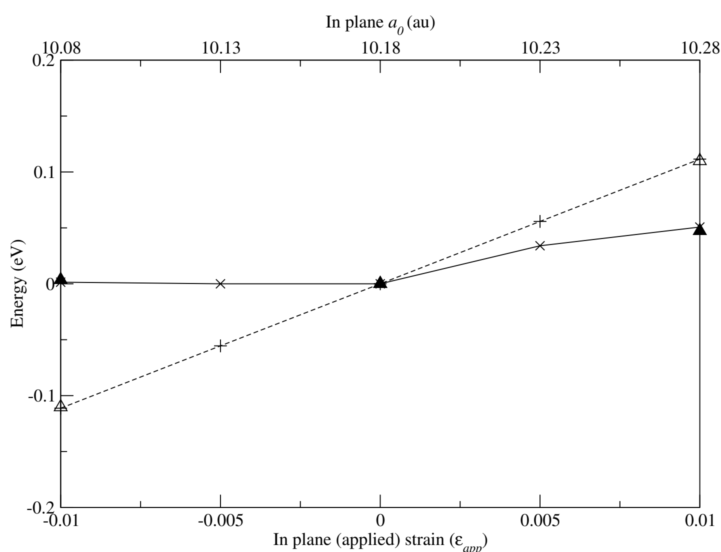

Figure 7. The formation energy of substitutional arsenic including and excluding the change in Fermi energy with strain. Plus signs joined by a dashed line and crosses joined by a solid line show values calculated using 64-atom supercells for the case where E_F is constant and where E_F varies with strain respectively. Empty triangles and filled triangles show the values where E_F is constant and where E_F varies with strain respectively calculated with 216-atom supercells to demonstrate convergence.

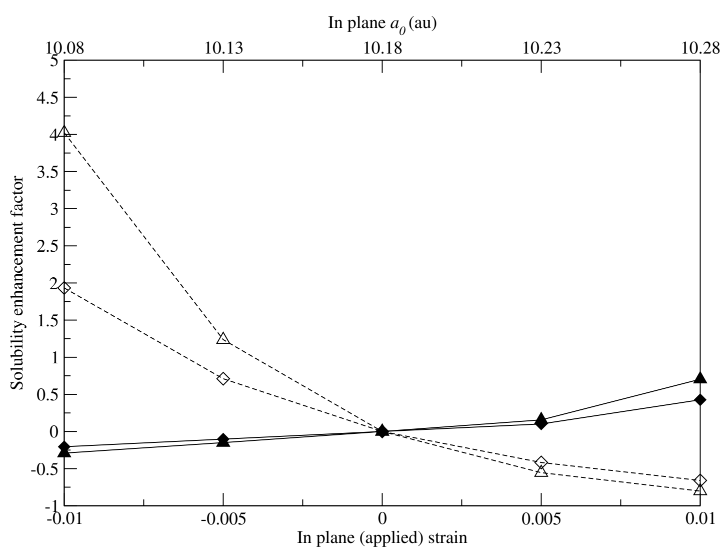

Figure 8. The enhancement to the equilibrium solubility of arsenic with strain for two different temperatures (triangles correspond to 800 K and diamonds correspond to 1200 K). To illustrate the influence of the change in Fermi energy the enhancement is shown for a Fermi energy set to be constant with strain (dashed lines and empty symbols) and for the value of E_F calculated as a function of strain (solid lines and filled symbols).

change in Fermi energy with strain is shown for arsenic in figure 7. The enhancement to the ESL is shown in figure 8. The effect of the Fermi energy is far more critical for arsenic. When the strain dependence of the Fermi energy is neglected the solubility of arsenic increases for

compressive strains, despite the fact that the arsenic atom has a larger atomic radius than a silicon atom. This is due to the fact that arsenic actually leads to a reduction in the overall silicon lattice constant as discussed above and hence compressive strain leads to a reduction in the total energy of the substitutional donor. It is the change in Fermi energy with strain that results in an increase in solubility of arsenic with tensile strain.

4. Discussion and conclusions

In agreement with previous theory [4] the equilibrium solubility limit of boron is significantly increased by compressive biaxial strain. The increased stability of the substitutional acceptor under compressive strain is due partly to a reduction in total energy but largely due to the increase in Fermi energy. Due to its opposite charge state, the change in Fermi energy with strain strongly increases the stability of arsenic in material under tensile biaxial strain. This enhancement is reduced by the fact that due to a negative value of β for arsenic, the total energy of substitutional arsenic is increased by tensile strain. The overall result is a small but significant enhancement to the solubility of substitutional arsenic strain in material subject to tensile biaxial strain. It is important to note that the change in Fermi energy with strain has been shown to play the dominant role in the determination of the solubility for both impurities in biaxially strained material.

References

[1] Cowern N E B, Zalm P C, van der Sluis P, Gravesteijn D J and de Boer W B 1994 Diffusion in strained Si(Ge) *Phys. Rev. Lett.* **72** 2585–8
[2] Rajendran K and Schoenmaker W 2001 Studies of boron diffusivity in strained $Si_{1-x}Ge_x$ epitaxial layers *J. Appl. Phys.* **89** 980–7
[3] Zangenberg N R, Fage-Pedersen J, Lundsgaard Hansen J and Nylandsted Larsen A 2003 Boron and phosphorus diffusion in strained and relaxed Si and SiGe *J. Appl. Phys.* **94** 3883–90
[4] Sadigh B, Lenosky T J, Caturla M-J, Quong A A, Benedict L A, Diaz de la Rubia T, Giles M M, Foad M, Spataru C D and Louie S G 2002 Large enhancement of boron solubility in silicon due to biaxial stress *Appl. Phys. Lett.* **80** 4738–40
[5] Monkhorst H J and Pack J D 1976 Special points for Brillouin-zone integrations *Phys. Rev.* B **13** 5188–92
[6] Cardona M and Christensen N E 1987 Acoustic deformation potentials and heterostructure band offsets in semiconductors *Phys. Rev.* B **35** 6182–94
[7] Cardona M and Christensen N E 1987 Acoustic deformation potentials and heterostructure band offsets in semiconductors *Phys. Rev.* B **36** 2906 (erratum)
[8] Hirth J P and Lothe J 1968 Theory of dislocations *Materials Science and Engineering* (New York: McGraw-Hill)
[9] Sze S M 1981 *Physics of Semiconductor Devices* 2nd edn (New York: Wiley–Interscience) pp 16–27
[10] Koteski V, Ivanovic N, Haas H, Holub-Krappe E and Mahnke H-E 2003 Lattice relaxation around impurity atoms in semiconductors—arsenic in silicon—a comparison between experiment and theory *Nucl. Instrum. Methods* B **200** 60–5
[11] Cargill G S III, Angilello J and Kavanagh K L 1988 Lattice compression from conduction electrons in heavily doped Si:As *Phys. Rev. Lett.* **61** 1748–51